MDPI

Article

Evolution and Predictive Analysis of Spatiotemporal Patterns of Habitat Quality in the Turpan–Hami Basin

Yaqian Li [1,2], Yongqiang Liu [1,2,*], Yan Qin [1,2], Kun Zhang [1,2], Reifat Enwer [1,2], Weiping Wang [1,2] and Shuai Yuan [3]

[1] College of Geography and Remote Sensing Sciences, Xinjiang University, Urumqi 830017, China; liyaqian@stu.xju.edu.cn (Y.L.); qinyan0215@xju.edu.cn (Y.Q.); zkun_@stu.xju.edu.cn (K.Z.); 107556522157@stu.xju.edu.cn (R.E.); 107556523168@stu.xju.edu.cn (W.W.)
[2] Xinjiang Key Laboratory of Oasis Ecology, Xinjiang University, Urumqi 830017, China
[3] School of Remote Sensing and Information Engineering, Hubei LuoJia Laboratory, Wuhan University, Wuhan 430079, China; yshuai@whu.edu.cn
[*] Correspondence: liuyq@xju.edu.cn

Abstract: The expansion of urban areas and unsustainable land use associated with human activities have brought about a decline in habitat quality (HQ), especially in arid regions with fragile ecosystems. A precise prediction of land use and habitat quality changes across different scenarios is crucial for the sustainable maintenance of ecological diversity. In this article, the InVEST model was employed to assess both the quality and degradation levels of habitats in the Turpan–Hami Basin (THB) spanning 1990~2020. Additionally, the InVEST-PLUS coupling model was employed to forecast habitat conditions under three different scenarios in 2050. Specifically, it involved the comparison of land use changes and spatial distribution of HQ across natural development (ND) scenarios, town development (UD) scenarios, and ecological protection (EP) scenarios, along with the analysis of hot spots of HQ spanning 1990~2050. The outcomes revealed the following: (1) The primary land use in the THB was categorized as unused land, alongside notable expansions in cultivated land, grassland, and built-up land. Conversely, there was a considerable decline observed in forests, water bodies, and unused land spanning 1990~2020. (2) The HQ within the THB exhibited evident spatial clustering characteristics. Between 1990 and 2020, areas with low HQ accounted for over 85%, areas with unchanged HQ constituted 88.19%, areas experiencing deteriorated HQ comprised approximately 5.02%, and areas displaying improved HQ encompassed around 6.79%. (3) Through the comparison of HQ for the ND, UD, and EP scenarios in 2050, it was observed that the average HQ under the EP scenario ranked highest, exhibiting the lowest degree of degradation on average. This indicates that the EP scenario is most advantageous for preserving HQ. Conclusively, this research provides valuable viewpoints for making decisions aimed at enhancing HQ in ecologically fragile arid regions.

Keywords: habitat quality; PLUS model; InVEST model; Turpan–Hami Basin

1. Introduction

Ensuring the availability of ecosystem services is paramount for human welfare [1–3], and the United Nations Decade for Ecosystem Restoration (2021–2030) is committed to advancing the preservation and rehabilitation of ecosystems globally. This endeavor aims to enhance the benefits that humans and nature derive from these ecosystems while restoring their service capacities [4]. HQ degradation due to unsustainable land use practices is a major global concern [5–8]. HQ refers to an ecosystem's capacity to furnish conducive conditions for the sustained survival and growth of individuals and populations. It serves as a representation of natural value and the ecosystem's ability to provide ecological services [9–11]. It can reflect ecological health and regional biodiversity status to a certain extent. In recent years, the excessive exploitation of ecological resources driven by the demands of economic development has caused degraded ecological functions and significant alterations in the spatial structure of land use [12], thereby exerting a substantial impact on

regional habitats. Changes in land use have been demonstrated to be a significant determinant in the modification of HQ, subsequently impacting the ecological milieu and regional biodiversity [13–15]. Recently, it has been emphasized that multi-scenario simulation can effectively unveil the potential problems and conflicts related to regional HQ under future land use changes. This approach serves as a foundation for making informed decisions for regional ecological management and promoting sustainable development [16,17].

Land use is the foundation of biodiversity, and its alteration stands as the most direct manifestation of human activities. Rational land utilization contributes to the enhancement of HQ. Therefore, predicting land use changes proves instrumental in implementing measures to avert deterioration in HQ. Based on current research, the methods for predicting land use changes mainly include dynamic simulation models that incorporate quantitative and spatial alterations, along with their hybrid counterparts. Common models include (1) the Markov model [18,19], which predicts the probability of future land use variations by analyzing historical data based on state transition probabilities; (2) the cellular automaton (CA) and its improved model [20,21], which simulate the dynamic process across land use variations using discrete space–time cellular units; (3) the system dynamics model (SD) [22], which describes the behavior or characteristics of the land use variations over time through simulation calculations based on interaction and feedback mechanisms between various system components; and (4) the patch generation land use simulation model (PLUS) [23–25], a combination of the Markov model and CA that considers both spatial and quantitative changes to simulate land use variations. The PLUS model, among the aforementioned models, is a combination of random forest and cellular automata, exhibiting superior simulation accuracy [26], comprehensive functionality, convenient operation, and excellent user experience. It has been extensively applied in land use change research. For instance, Meimei, et al. [27] employed the PLUS model to predict the land use types and conflicts in Xining City from 2020 to 2030 under different scenarios, and believed that the expansion trend of construction land in the core area and peripheral areas was similar. However, the reduction in cultivated land in the peripheral areas was notably more pronounced. Through assessing both absolute and relative land use conflicts, they proposed sustainable development strategies. Gao et al. [28] utilized the PLUS model to simulate the land use in Nanjing across four scenarios encompassing commercial normality, rapid economic development, ecological protection, and ecological-economic balance. They acquired the ecological risks associated with land use under different scenarios and designed different development models to mitigate these risks based on the outcomes of ecological risk assessment.

Because HQ represents biodiversity and ecosystem services, its assessment has received significant attention from geographers and ecologists. To date, a variety of methodologies and tools have been employed for evaluating HQ, including Social Values for Ecosystem Services (SolVES) [29,30], Soil and Water Assessment Tool (SWAT) [31,32], the Integrated Valuation of Ecosystem Services and Tradeoffs (InVEST) model, etc. The InVEST model is capable of capturing the spatial heterogeneity of HQ with minimal parameters and presenting results in a visually appealing manner. Consequently, it has been widely utilized for quantitative research on HQ. For instance, Chen et al. (2023) [33] employed the InVEST model to assess the changes in HQ within the fern forest area of the Mohe River basin located in the western Tianshan Mountains and then analyzed the factors influencing HQ. Their findings indicated an increase in fragmentation within the study area, with low habitat value observed in areas prone to geological disasters and human activity interference. Zhang and Chen (2022) [34] employed the InVEST model to evaluate and simulate the HQ within the Tarim River basin and proposed suggestions for land use planning and protection on the basis of evaluation results. Therefore, the InVEST model can be used to quantify HQ, enabling deci-sion-makers to effectively evaluate the societal implications of land use alterations (Wang et al. 2022) [35]. This approach provides a scientific foundation and decision support for professionals engaged in land use planning and management. In the context of future predictions or multi-scenario simulations, numerous scholars have

achieved promising results using the PLUS-InVEST model. For example: Wei et al. [36] utilized the PLUS-InVEST model to assess the HQ and degradation level of Aibi Lake Basin in Xinjiang from 1990 to 2030, which facilitated the establishment of ecological zoning based on evaluation outcomes. Wang et al. [37] utilized the PLUS-InVEST model to assess the HQ of three distinct compact urban scenarios in 2040 and 2060 within the Guangdong–Hong Kong–Macao Greater Bay Area. Their results revealed a significant decline in urban HQ under the highly compact scenario, emphasizing the need for collaborative efforts toward ecological protection and sustainable development. Liu et al. (2023) [38] applied the GMOP-PLUS-InVEST model to simulate land use/land cover changes and evaluate water yield in the Nansi Lake Basin, China. Their study conducted multi-scenario simulations to explore how different land use changes impact water resources, providing insights into sustainable land and water management practices in the region. Li et al. (2023) [39] utilized the PLUS-InVEST model to analyze the spatial distribution of ecosystem carbon storage in Liaoning Province, China. Their results highlighted significant variation in carbon storage, with higher concentrations in forested and wetland areas, and lower levels in anthropogenically impacted regions. The study identified land use and climate as key drivers of carbon storage patterns, offering insights for optimizing land management to enhance carbon sequestration.

The Turpan–Hami Basin (THB) is a typical representative of an extremely arid area and extremely fragile ecological environment. This study comprehensively used 3S technology and the InVEST model to evaluate and analyze the HQ of the THB, predicted the HQ of the THB in 2050 with the PLUS model, and analyzed the cold hot spot of HQ from 1990 to 2050. According to the policy planning and advocacy suggestions during China's 14th Five-Year Plan period, three scenarios were established, namely the natural development (ND) scenario, town development (UD) scenario, and ecological protection (EP) scenario. By means of the PLUS model, the spatial distribution pattern of land use in the THB by 2050 was predicted and analyzed, and in combination with the InVEST model, the changes in HQ of the THB across different development scenarios were assessed. This research is processed with following objectives: (1) explore the spatio-temporal patterns of land use variations in the THB spanning 1990~2020; (2) assess the spatio-temporal patterns of HQ in the THB spanning 1990~2020; (3) predict the distribution difference in HQ across different future scenarios; (4) unravel the distribution law of HQ in the THB from 1990 to 2050 by analyzing its hot and cold spots.

2. Study Area and Data Sources

2.1. Study Area

The Turpan–Hami Basin (87°16′–96°23′ E, 40°52′–45°05′ N), located in the eastern part of the Xinjiang Uygur Autonomous Region, is recognized as one of China's largest land basins (Figure 1). Positioned between the northern foothills of the Tianshan Mountains and the southern foothills of the Altay Mountains, this basin boasts a relatively flat terrain. It comprises two distinct parts, the Turpan Basin and the Hami Basin, with a composite area of roughly 21×10^4 km^2, accounting for 12.6% of Xinjiang's total land area. The region encompasses six counties: Gaochang District, Shanshan County, Toxsun County, Yizhou District, Barkun County, and Yiwu County, with a total population of around 1.36 million. The region has a typical continental arid climate with large diurnal temperature differences, very low precipitation, and high evaporation [40], and shows an average annual rainfall in the range of 10 to 30 mm and an average annual potential evaporation of 3000 to 4000 mm. Frequent occurrences of gales and extremely high temperatures contribute to its complex ecosystem consisting of mountains, oases, and deserts [41]. The ecological environment within this basin is highly fragile, with desertification coexisting alongside wetland degradation, and ecological droughts pose significant challenges to restoration efforts. However, due to ongoing economic development coupled with societal progressions in recent years, great pressure has been placed on ecological restoration projects within the THB.
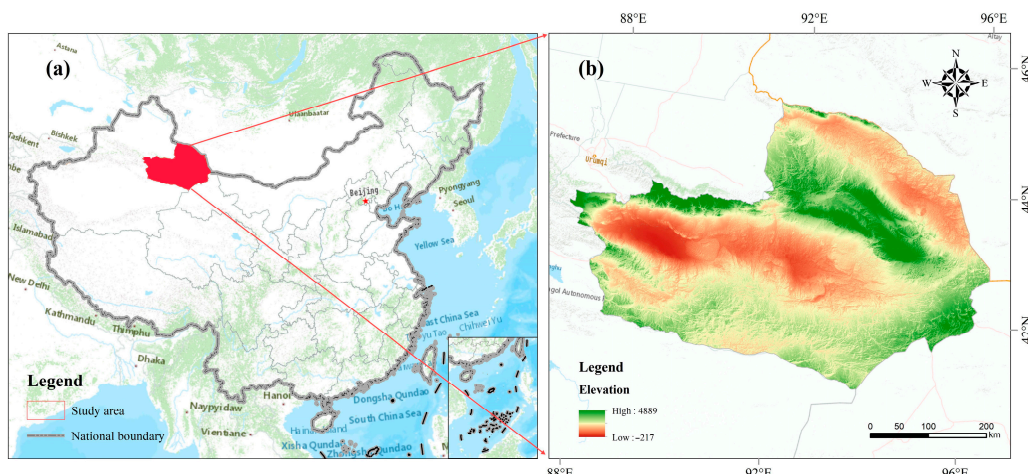
Figure 1. (**a**) Location of the study area in China and (**b**) elevation of the study area.

2.2. Data Sources

The study data mainly consist of various datasets encompassing digital elevation model (DEM), land use, soil, topographic, climate, road accessibility, and socio-economic data (Table 1). The land use data were sourced from the Institute of Resource and Environment Science and Data Center affiliated to Chinese Academy of Sciences, providing 30 m resolution land use data for the years 1990, 2000, 2010, and 2020.

Table 1. Data table.

Type	Data	Data Source	Resolution
Land Use Data	CAS-LULC	Resource and Environment Science and Data Center, Chinese Academy of Sciences (https://www.resdc.cn/ (accessed on 13 December 2022))	30 m
Natural Environment Indicators	DEM	National Geospatial Data Cloud (http://www.gscloud.cn/ (accessed on 13 December 2022))	30 m
	Slope	Based on ArcGIS10.8	30 m
	NPP	USGS (https://www.usgs.gov (accessed on 13 December 2022))	500 m
	NDVI	NASA (https://earthdata.nasa.gov/ (accessed on 13 December 2022))	
	Annual evapotranspiration data	National Tibetan Plateau Data Center (https://data.tpdc.ac.cn/home (accessed on 13 December 2022))	1 km
	Annual precipitation data		1 km
	Soil type	Soil dataset for China Based on the World Soil Database (HWSD) (https://iiasa.ac.at/models-tools-data/hwsd (accessed on 13 December 2022))	1 km
	Temperature	ERA5-Land dataset (https://cds.climate.copernicus.eu (accessed on 13 December 2022))	1 km
Human Activity Indicators	Nighttime light data	National Tibetan Plateau Data Center (https://data.tpdc.ac.cn/home (accessed on 13 December 2022))	500 m
	Population	World pop (https://hub.worldpop.org (accessed on 13 December 2022))	
	GDP	Statistical Yearbook	
Transportation Convenience Indicators	Distance from first-class road Distance from second-class road Distance from third-class road Distance from highway Distance from railway Distance from water Distance from the county seat	OpenStreetMap (https://www.openstreetmap.org/ (accessed on 13 December 2022))	

According to the requirements of accuracy and practicability for the PLUS model, three categories of indicators were selected, i.e., natural environment, transportation convenience, and human activity (Table 1), which included 18 driving factors affecting land use change, including elevation, net primary productivity (NPP), gross domestic product (GDP), normalized difference vegetation index (NDVI), population, rain, slope, temperature, and distance from roads. Distances to water bodies, county governments, and roads

were computed utilizing Euclidean distance of ArcGIS software. Then, all datasets were trimmed by the vector boundary of the THB, and the projection coordinate system and resolution were unified, followed by resampling to a resolution of 30 m.

3. Methods

3.1. HQ Assessment

This research utilized the InVEST model to assess the level of habitat degradation and HQ in the THB. The HQ module of the InVEST (3.13.0) model considers HQ as a biodiversity indicator linked to various land use types [42]. It assumes that areas with higher HQ are able to sustain a greater diversity of species, while a decrease in HQ will result in reduced biodiversity. The primary input data are composed of land use/cover, predominant threat factors, weight and impact distance of threat sources, and the sensitivity of land use/cover to each threat source. The parameters for the InVEST model were established in accordance with previous research [13,15,43], as shown in Tables 2 and 3. Using these parameters, we calculated the extent of habitat degradation and HQ in the THB across four time nodes: 1990, 2000, 2010, and 2020.

Table 2. Threat factor parameters.

Threat	Max_Dist (km)	Weight	Decay
Cultivated	4	0.6	linear
Rural *	5	0.8	exponential
Urban	8	1	exponential
Other construction *	7	0.8	exponential
Unused	4	0.4	linear

* represents threat factors not applied in the three scenarios for 2050.

Table 3. Sensitivity parameters of various land use types to habitat threat factors.

Land Use Type	Habitat Suitability	Threat Factors				
		Cultivated	Rural *	Urban	Other Construction *	Unused
Cropland	0.5	0	0.8	0.6	0.7	0.4
Forest	1	0.7	0.9	0.7	0.8	0.5
Grassland	0.9	0.8	0.7	0.75	0.75	0.7
Water	0.9	0.5	0.6	0.7	0.7	0.5
Built-up land	0	0	0	0	0	0
Unused	0.3	0.2	0.4	0.45	0.6	0

* represents threat factors not applied in the three scenarios for 2050.

First, the degree of the habitat degradation is calculated:

$$D_{xj} = \sum_{r=1}^{R} \sum_{y=1}^{Y_r} \left(\frac{w_r}{\sum_{r=1}^{R} w_r} \right) r_y i_{rxy} \beta_x S_{jr} \tag{1}$$

$$i_{rxy} = 1 - \left(\frac{d_{xy}}{d_{r\max}} \right) \tag{2}$$

$$i_{rxy} = \exp\left[-\left(\frac{2.99}{d_{r\max}} \right) d_{xy} \right] \tag{3}$$

where D_{xj} represents the index of habitat degradation; R represents the amount of threat factors; w_r represents the weight assigned to the threat factor r; Y_r represents the amount of grids affected by the threat factor r; r_y represents the value of the threat factor r on a specific grid; i_{rxy} represents the distance from the habitat to the threat source, as well as the

influence of threats on space; β_x represents factors that mitigate threats' impact on habitat according to different protection policies (e.g., legal protection degree, where 0 indicates no legal protection and 1 indicates full legal protection); S_{jr} represents the sensitivity of habitat type *j* to the threat factor *r*; d_{xy} denotes the Euclidean distance from grid *x* to grid *y*; and d_{rmax} signifies the longest distance at which a particular threat source can affect habitats. A higher score in the calculation reflects more significant degrees of threats posed by these factors towards habitats, indicating higher levels of habitat degradation.

Following the above results of HQ degradation, the HQ is evaluated as follows:

$$Q_{xj} = H_j \left[1 - \left(\frac{D_{xj}^Z}{D_{xj}^Z + k^z} \right) \right] \tag{4}$$

where Q_{xj} represents the HQ index of grid *x* in land use *j*; H_j denotes the habitat suitability of habitat type *j* ranging between 0 and 1; *k* is the semi-saturation constant, typically set as half the maximum value of the habitat degradation; and *Z* is the normalized constant, usually set to 2.5.

3.2. Prediction of Land Use Changes in Future

The Patch-generating Land Use Simulation (PLUS) model is a novel land use simulation model designed by [44] at China University of Geosciences, based on the enhanced CA model. It can simulate the changes in land use resulting from patches, providing benefits for investigating the drivers of such changes and dynamically simulating diverse land use types, particularly patch alterations in forests and grassland. The PLUS model primarily consists of two components, the land expansion analysis strategy module (LEAS) as well as the CA module utilizing various types of random patch seeds (CARS).

LEAS employs the random forest algorithm to mine various types of land use expansion and their corresponding driving force factors, followed by the calculation of likelihood of the development for each land use type and the quantification of impact of specific driving factors on the expansion of each land use type during the given period. This module preserves the capability of the model to dissect the mechanism underlying land use changes within a defined timeframe and demonstrates versatility in its application. On the other hand, CARS integrates random seed generation with the threshold-decreasing mechanism. Building upon the probability maps generated by the LEAS module, not only can it predict the likelihood of development for different land use types, but the spatial distribution of land use patterns can also be simulated. CARS operates as a scenario-based land use simulation model, providing insights into potential future land use scenarios.

3.2.1. Multi-Scenario Simulation Setting

Based on previous research findings, the parameters such as domain weight within the PLUS model were determined [32,39,44]. Subsequently, land use simulations for three scenarios in 2050 were conducted. The ND scenario served as the benchmark scenario in this study. In this particular scenario, the historical trend in land use changes spanning 1990~2020 was preserved, and predictions for land use in 2050 were generated using the PLUS model's Markov chain module. The objective of the UD scenario is to enhance the level of urbanization, expand urban infrastructure, restrict the conversion of urban land into other land categories, and promote the transformation of unused and underutilized land into urban construction zones. The EP scenario aims to safeguard regions with high-quality habitats by strictly limiting conversions from water bodies, forests, and grasslands to cultivated or developed lands while controlling excessive expansion in these areas. Additionally, it seeks to unlock the developmental potential of forests and grasslands. The PLUS model was employed for predicting species-specific changes in distribution under the ND scenario as well as across both UD and EP scenarios.

3.2.2. Model Validation

To ensure the model simulation accuracy, this study utilized the land use data of 2010 as the baseline. By incorporating 18 driving factors specific to the THB, we conducted simulations and forecasts for the land use data up to 2020. Subsequently, a comparison was made between the PLUS model-generated THB land use map and the factual THB land use map in 2020. The reliability of the PLUS model simulation was evaluated using the Kappa coefficient [39].

3.3. Analysis of Spatial Data Hot Spots

A 5 km×5 km grid network of fishing points was established within the study area. Using ArcGIS extraction tools, grid values were extracted to points for hot spot analysis (Getis-Ord Gi*). A detailed investigation was conducted focusing on hot spots with statistical significance and confidence levels exceeding 90%. Utilizing the ArcGIS platform, spatial clustering and distribution characteristics of the HQ index in the THB were analyzed, revealing the spatial distribution patterns of the HQ index in the THB.

4. Results

4.1. Analyses of Land Use Changes Spanning 1990 to 2020

The land use changes spanning 1990 to 2020 are depicted in Figure 2. By 2020, the THB is predominantly characterized by unused land, constituting 78.81% of the total land use area. Grassland is the second largest land use type, comprising 18.81% of the area, while other land use classes have a minor share, accounting for less than 3% of the total. This distribution can be explained by the unique terrain of the THB, where the limited oasis areas result in grasslands and forests primarily distributed along the Bogda Mountains in the eastern segment of the Tianshan Mountains. To visually analyze the land use changes during the study period, a visualization analysis of its transition matrix was conducted (Figure 3). Overall, 89.3% of land use classes remained unchanged. Among them, farmland increased by a total of 1117.57 km^2 over the past three decades; forest land shows a consistent decreasing trend, with the largest reduction of 224 km^2 observed between 2000 and 2010 and a total decrease of 256.33 km^2; grassland exhibits a trend of decreasing and then increasing, notably growing between 2000 and 2010, with a total increase of 7873.40 km^2 in the past three decades; water bodies show a fluctuating decreasing trend, with an overall reduction of 67.30 km^2; urban areas experience a continuous increase, totaling an increment of 708.05 km^2; and unused land exhibits a continuous decrease, with a total reduction of 9375.39 km^2. From Figure 4, it can be observed that the increase in grassland primarily originates from previously unused land, and grassland is mainly concentrated around mountain ranges, including the Bogda Mountains in the eastern part of the Tianshan Mountains and the Jueluotage Mountains in the central branch of the Tianshan Mountains. The increase in farmland mainly comes from grassland and unused land, and farmland is predominantly distributed around urban areas.
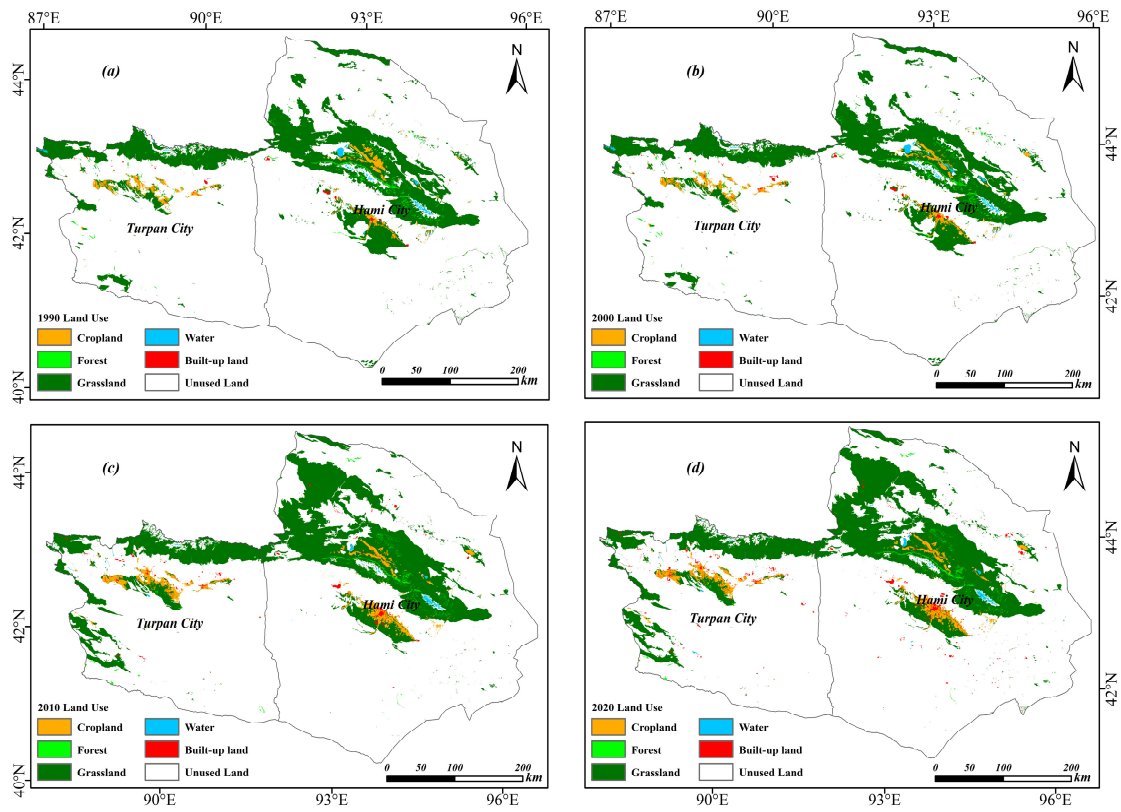
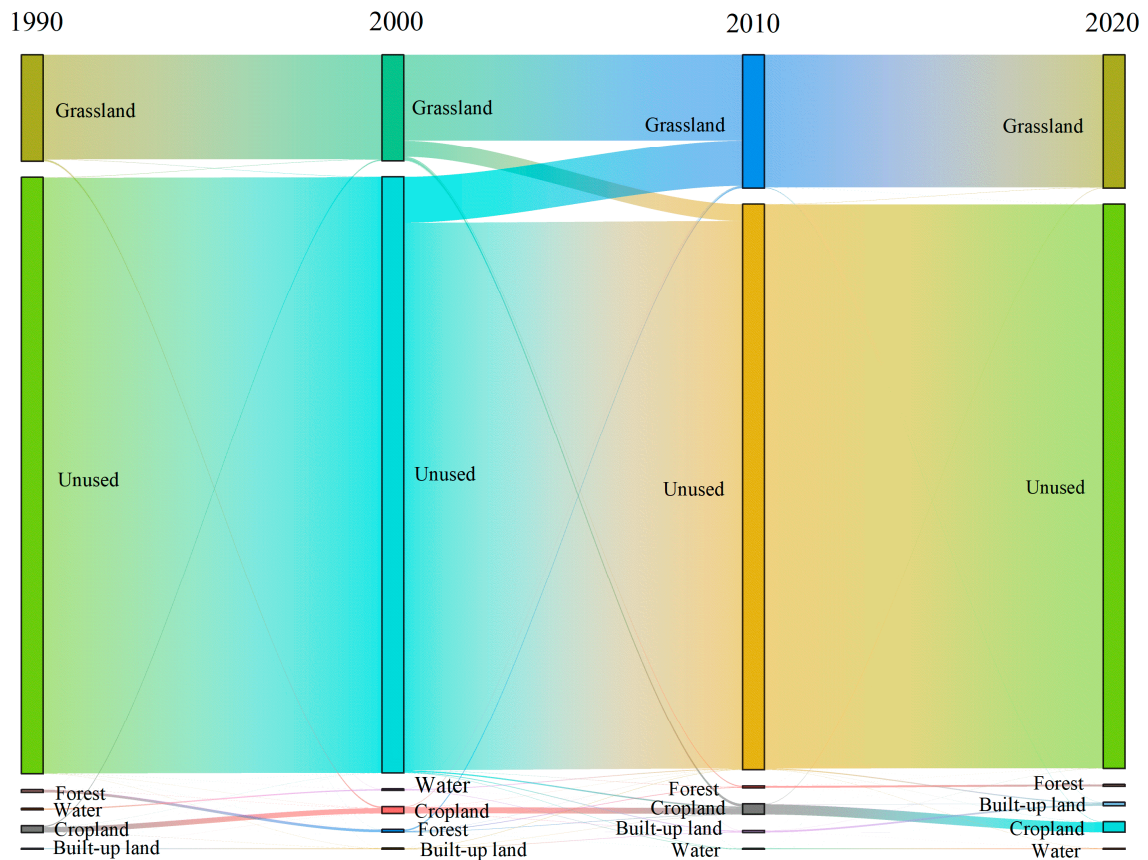**Figure 2.** Land use types in different times: (**a**) 1990, (**b**) 2000, (**c**) 2010, and (**d**) 2020.
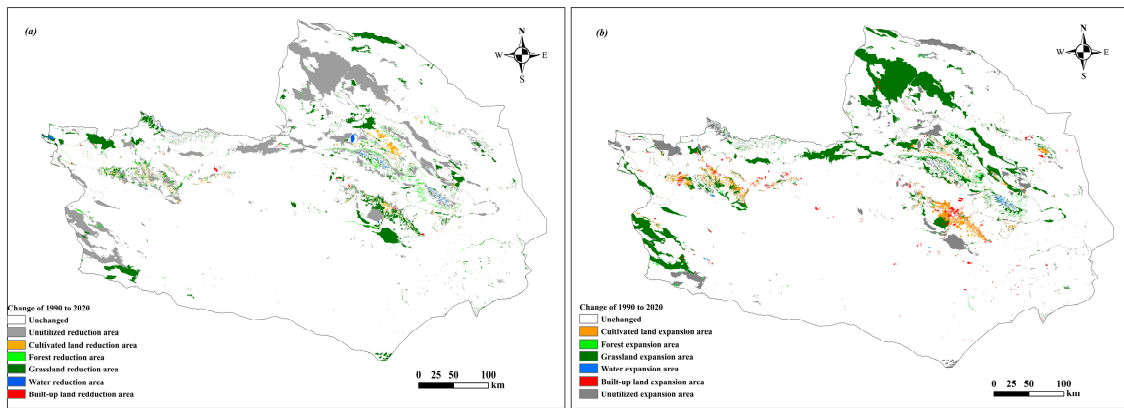

**Figure 3.** Sankey map of land use changes in THB spanning 1990~2020.

Figure 4. (**a**) Area decrease and (**b**) area increase of land use types in THK spanning 1990~2020.

4.2. Spatio-Temporal Evolution of Habitat Degradation Spanning 1990 to 2020

Within the InVEST model, a habitat degradation index is usually adopted to quantify the habitat degradation extent. Figure 5 illustrates the extent of habitat degradation in the THB spanning 1990~2020. The majority of areas have remained unaffected by degradation, primarily consisting of unused land types. To quantify the habitat degradation in the THB, the study divided the habitat degradation extent into five grades (Figure 6), i.e., low (0–0.1), below average (0.1–0.2), moderate (0.2–0.3), above average (0.3–0.4), and high (>0.4). Specifics of the change in habitat degradation extent spanning 1990 to 2020 are as follows: 199,537.31 km^2 areas in the THB remain unchanged, accounting for 96.41% of the total area; 5420.40 km^2 areas show an increased degradation extent, accounting for 2.62% of the total area; and 2045.56 km^2 areas exhibit a decreased degradation extent, accounting for 0.97% of the total area. The habitat degradation areas are mainly concentrated around the cities, and the overall trend in degradation is aggravated.
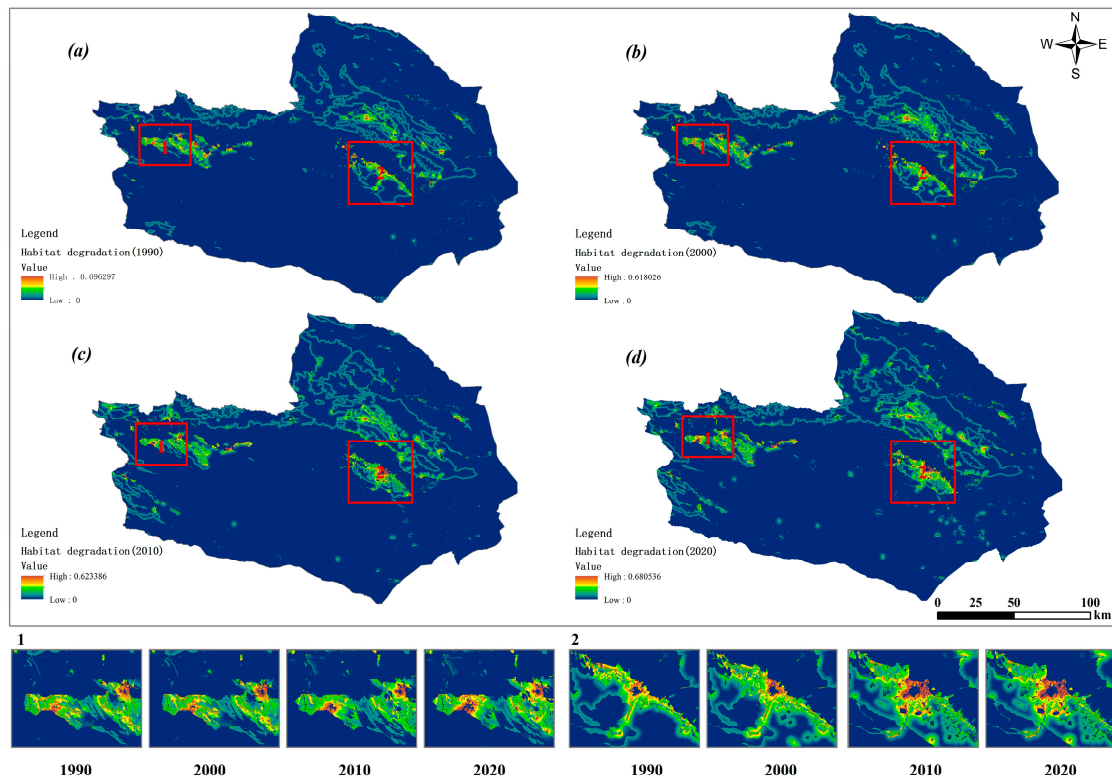
Figure 5. Habitat degradation maps in THB at different times: (**a**) 1990, (**b**) 2000, (**c**) 2010 and (**d**) 2020; Bold 1, 2 represent two sample areas.
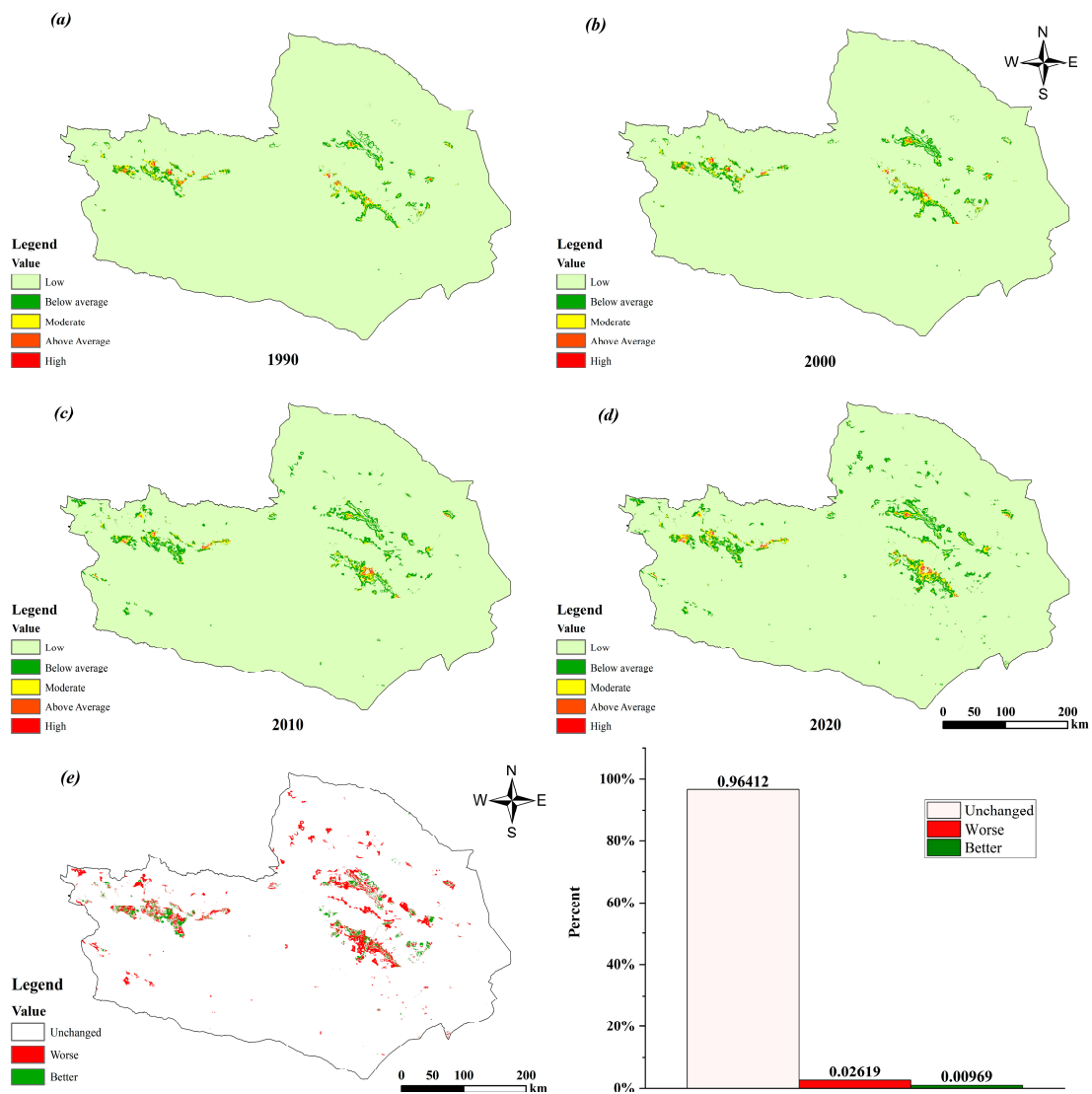
Figure 6. Extent of habitat degradation in THB at different times: (**a**) 1990, (**b**) 2000, (**c**) 2010, and (**d**) 2020. (**e**) Changes in habitat degradation during 1990–2020.

4.3. Spatio-Temporal Evolution of HQ Spanning 1990 to 2020

Based on the InVEST model, the HQ Index was employed to assess the condition of HQ. The HQ Index demonstrates a spectrum of values ranging between approximately 0 and 1, with a higher value suggesting improved habitat quality, thereby fostering biodiversity conservation. Following the natural break method, the HQ in the study area was categorized into four levels [36,45], i.e., poor (0–0.25), fair (0.25–0.5), moderate (0.5–0.75), and high (0.75–1). As illustrated in Figure 7, the HQ in the THB spanning 1990~2020 shows no significant spatial variation in most areas. The average HQ Index decreases from 0.112 in 1990 to 0.110 in 2000, increases to 0.129 in 2010, and then declines to 0.126 in 2020. According to the HQ levels in 2020, regions classified as high, moderate, and fair HQ levels are predominantly characterized by grassland, accounting for 96.44%, 98.72%, and 92.76% of the overall land areas, respectively. Conversely, the primary land use type in areas categorized as poor HQ level is unused land, constituting 91.11%. In terms of land use classification, 84.19% of arable land is distributed in areas categorized as poor HQ, with the remainder in fair-quality regions. Forest land is predominantly distributed in high-quality areas, representing 45.95%, with the rest spread across various levels. Grassland accounts for 31.32% and 30.17% in regions with poor and moderate quality levels, respectively.

Meanwhile, urban land and unused land almost exclusively occupy poor quality level regions, nearly reaching 100% in distribution.
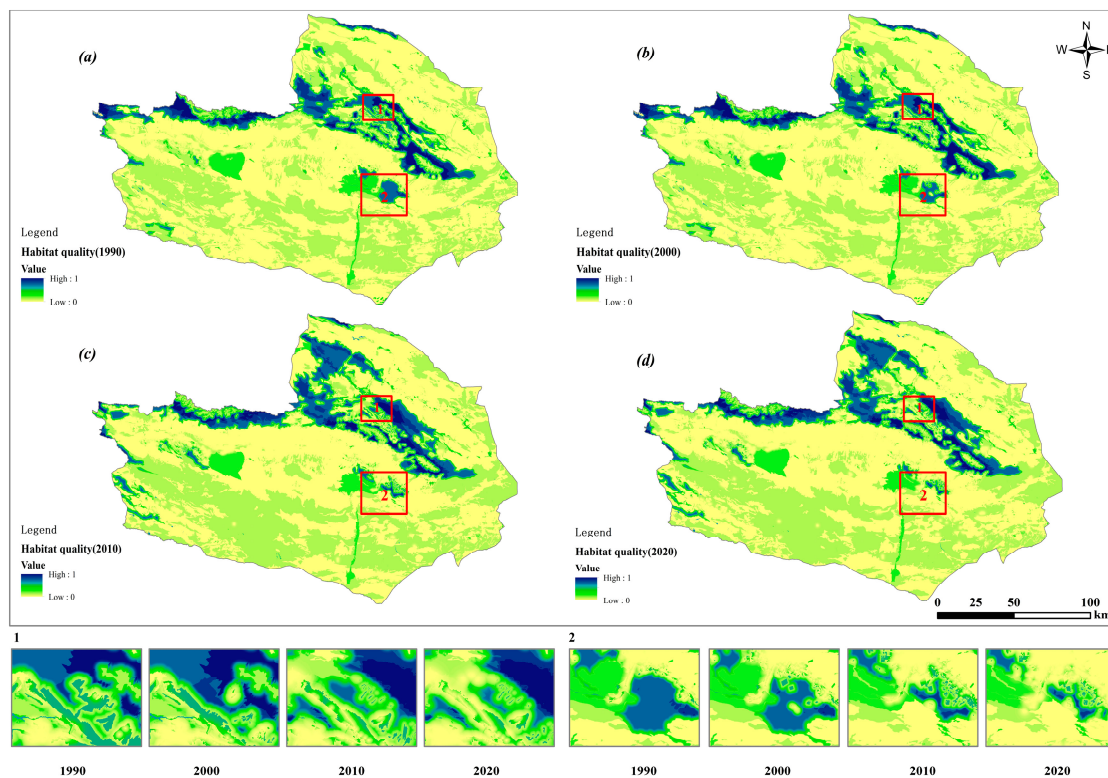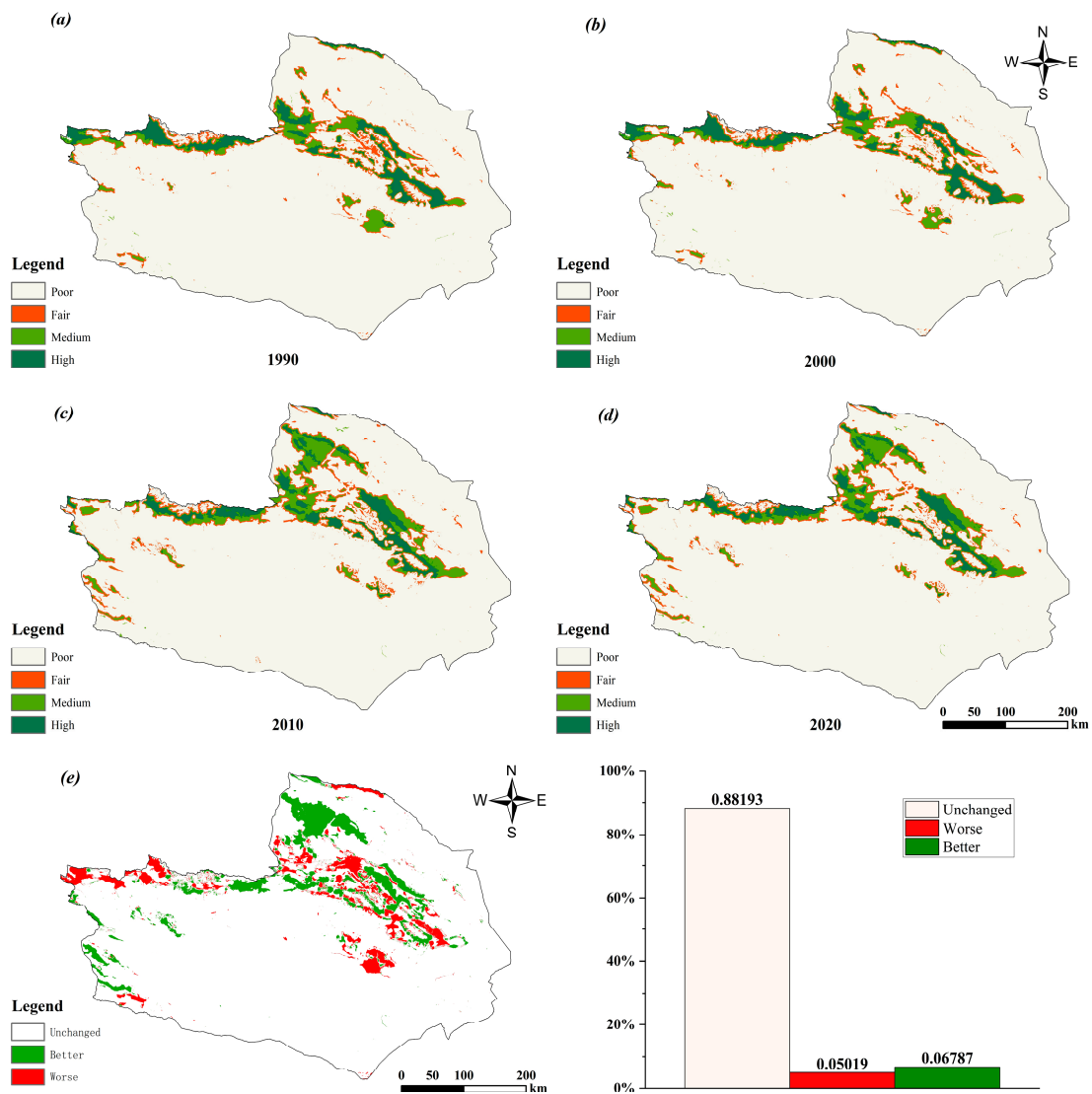

Figure 7. HQ levels in THB at different times: (**a**) 1990, (**b**) 2000, (**c**) 2010 and (**d**) 2020; Bold 1, 2 represent two sample areas.

The HQ levels spanning 1990~2020 (Figure 8) and their corresponding area changes are presented in Table 4. The area of habitats categorized as poor quality decreased by 3808.2 km^2, while the area of moderate-quality habitats increased by 3493.06 km^2. Changes in the areas classified as fair and high-quality are relatively minimal. Notably, throughout the period spanning 1990~2020, areas designated as poor-quality habitats consistently account for over 85% of the total area. Areas with unchanged HQ levels cover 88.19% of the total area, while areas with decreased HQ levels account for 5.02%, and those with improved HQ levels constitute 6.79%. Consistent with spatial patterns of land use, areas characterized by poor HQ levels are primarily concentrated within desert regions and urban built-up areas, while areas with high HQ levels are predominantly distributed along mountainous terrains.

Table 4. Specific data of areas across HQ levels spanning 1990~2020.

HQ Level	1990		2020		Changes in Areas Spanning 1990~2020	
	Area/km^2	Proportion/%	Area/km^2	Proportion/%	Area/km^2	Proportion/%
Poor	183,319.13	0.8857	179,510.93	0.8673	−3808.2	−0.0184
Fair	7657.38	0.0369	7937.19	0.0383	279.81	0.0014
Moderate	8281.93	0.0400	11,774.99	0.0569	3493.06	0.0169
High	7712.45	0.0373	7748.28	0.0374	35.83	0.0002

Figure 8. HQ levels in THB at different times: (**a**) 1990, (**b**) 2000, (**c**) 2010, and (**d**) 2020; (**e**) HQ variations spanning 1990~2020.

4.4. Predictions for Three Scenarios in 2050

In this study, the Kappa coefficient for the validation of the PLUS model was 0.8762, suggesting the simulation results could meet the research needs. Using the PLUS model, the land use changes in the THB for the year of 2050 under three scenarios, namely ND, UD, and EP scenarios, were simulated and predicted. The simulation results provide distinct distribution patterns for the three scenarios.

4.4.1. Land Use Predictions for Three Scenarios in 2050

Based on the land use data in the year 2020, the PLUS model was employed to predict the land use data in 2050. Figure 9 illustrates the land use types distribution pattern for the year of 2050 across the three scenarios, while Table 5 displays the land use types in the THB corresponding to these scenarios. Under the ND scenario, the alterations in data for various land use types from 2020 to 2050 are as follows: except for the unused land, the rest land types have an increasing trend in varying degrees. Among them, the built-up land has the largest increase, increasing by 943.80 km^2, the forest increases by 26.82 km^2, the grassland increases by 76.91 km^2, the water area increases by 81.45 km^2, while the unused land decreases by 1042.81 km^2. In the EP scenario, taking the ND scenario in 2050 as a reference, the cultivated land increases by 792.68 km^2, the forest increases by 93.63 km^2,

the grassland increases by 720 km^2, and the water area increases by 142 km^2. On the contrary, the built-up land and unused land decreases by 319.20 km^2 and 1429.11 km^2, respectively. In the UD scenario, taking the ND scenario in 2050 as a reference, the built-up land increases by 832.99 km^2, and the unused land decreases by 900 km^2. For each of the three scenarios in 2050, the percentage of unused land in the total land use area remains the highest, reaching over 78%, with the EP scenario exhibiting the highest utilization rate for such land. In comparison to 2020, cultivated land decreases under both the ND and UD scenarios, while it increases under the EP scenario. Across all scenarios in 2050, there is an overall increase in water areas, particularly noticeable within the ecological scenario. Additionally, built-up land experiences significant expansion across all scenarios, with the UD scenario showcasing the most pronounced growth.
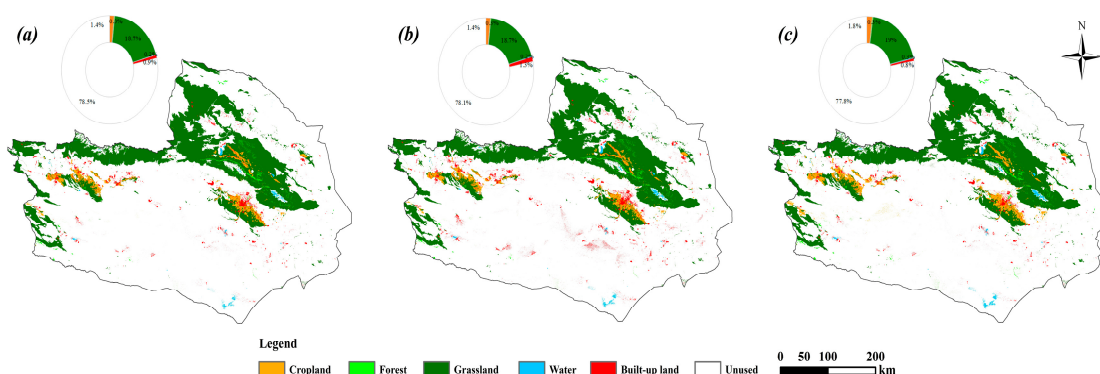

Figure 9. Land use type distribution for the (**a**) ND, (**b**) UD, (**c**) EP scenarios in 2050.

Table 5. Areas of land use types for the three scenarios in 2050.

| Land Use Type	ND Scenario in 2020		ND Scenario in 2050		UD Scenario in 2050		EP Scenario in 2050	
	Area/km^2	Proportion/%	Area/km^2	Proportion/%	Area/km^2	Proportion/%	Area/km^2	Proportion/%
Cropland	3052.66	1.47	2966.41	1.43	2966.41	1.43	3759.09	1.82
Forest	568.24	0.27	595.06	0.29	592.07	0.29	688.69	0.33
Grassland	38,523.84	18.61	38,600.75	18.65	38,600.75	18.65	39,320.75	19.00
Water	301.37	0.15	382.84	0.18	452.84	0.22	524.84	0.25
Built-up land	977.18	0.47	1920.98	0.93	2753.96	1.33	1601.77	0.77
Unused land	163,547.60	79.02	162,504.79	78.52	161,604.79	78.08	161,075.68	77.83

The trends in different land use types are consistent with the scenarios, showcasing the impacts of urbanization and economic development on natural resources, as well as the sustainable development of resources under ecological conservation scenarios. These trend analyses provide an understanding of various land use type changes across different land use scenarios, which helps guide future land planning and sustainable development decisions.

### 4.4.2. Habitat Degradation and HQ Analysis

The habitat degradation across different scenarios for the year 2050 is depicted in Figure 10. Overall, the average degradation degree stands at 0.071 under the ND scenario, 0.079 under the UD scenario, and 0.068 under the EP scenario. The highest level of degradation occurs under the UD scenario.

The HQ across different scenarios in 2050 is illustrated in Figure 11. The average HQ under the ND scenario is 0.219, which is 0.201 lower than the UD scenario and 0.223 lower than the EP scenario. The EP scenario exhibits the highest HQ. Across the three scenarios, areas with poor and fair HQ account for over 80% of the total land. The most significant changes occur in areas with lower HQ, whereas areas with moderate or higher HQ remain distributed along the mountain ranges with less noticeable variations. From Figure 11d,

HQ levels decrease in the UD scenario compared to the ND scenario, with a shift in most regions from a fair to a poor quality rating. Additionally, Figure 11e shows an improvement in HQ under the EP scenario compared to the NP scenario, with a major transition from poor to fair quality levels.
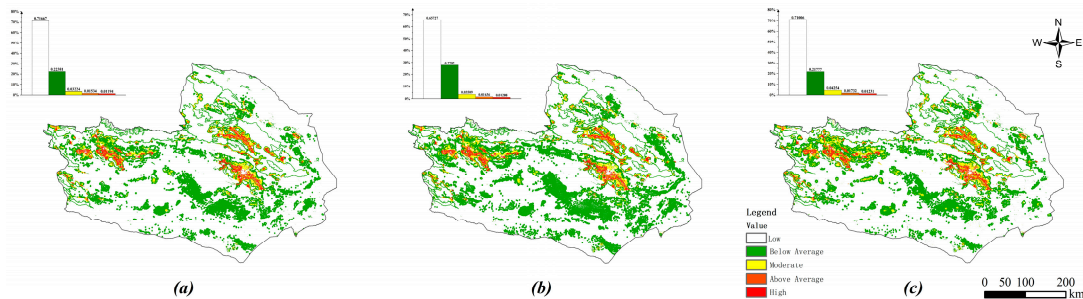
**Figure 10.** Habitat degradation levels and proportions under three scenarios in 2050: (**a**) ND, (**b**) UD, (**c**) EP.
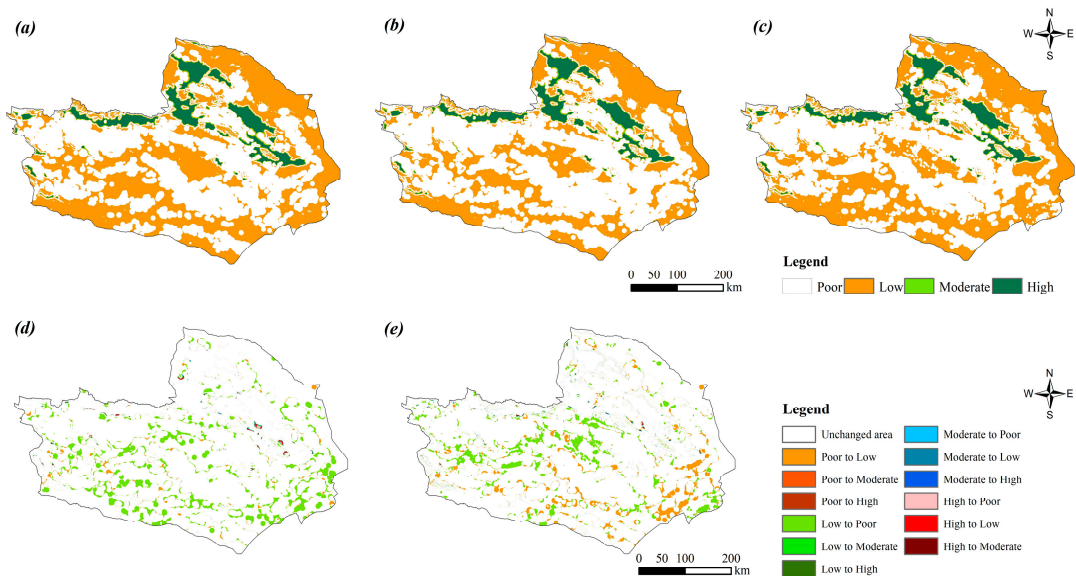
Figure 11. HQ classification chart for three scenarios in 2050: (**a**) ND; (**b**) UD; (**c**) EP. (**d**) Comparison of HQ between ND scenario and UD scenario; (**e**) comparison of HQ between ND scenario and EP scenario.

4.5. Contribution Analysis

The land use expansion analysis module within the PLUS model employs a strategy to extract and analyze different land use expansions between two periods of change. It then samples from the increased portion and identifies the factors contributing to these expansions using the random forest algorithm. This process enables the determination of the likelihood of the development for different land uses and the quantification of the impact of driving forces on their expansion during this period. Taking the land use data of 2020 as an example, the contributions of 18 driving factors to land expansion during this period are presented in Figure 12. The most significant factor for cultivated land is NDVI, contributing approximately 13.61%, followed by the human activity index with a contribution of about 12.42%. The third influential factor is potential evapotranspiration, contributing around 8.03%. For forests, DEM emerges as the primary driver with a substantial impact of approximately 16.66%, closely followed by potential evapotranspiration with about 13.35%. Rainfall stands out as the dominant factor affecting grassland with a contribution of roughly 13.16%. Both DEM and potential evapotranspiration play a crucial role in the expansion

of water bodies, contributing approximately 9.37% and 10.51%, respectively. The human activity index exhibits the highest impact on built-up land, accounting for about 36.79% of its expansion rate while rainfall takes precedence in influencing unused land at around 13.42%. It should be noted that precipitation has a significant impact and contribution of over 5% across all types of land uses. In particular, its impact on unused land and grassland is more pronounced compared to cultivated areas, where its influence is comparatively less. The combined average contribution of precipitation and potential evapotranspiration to all types of land reaches 17%.
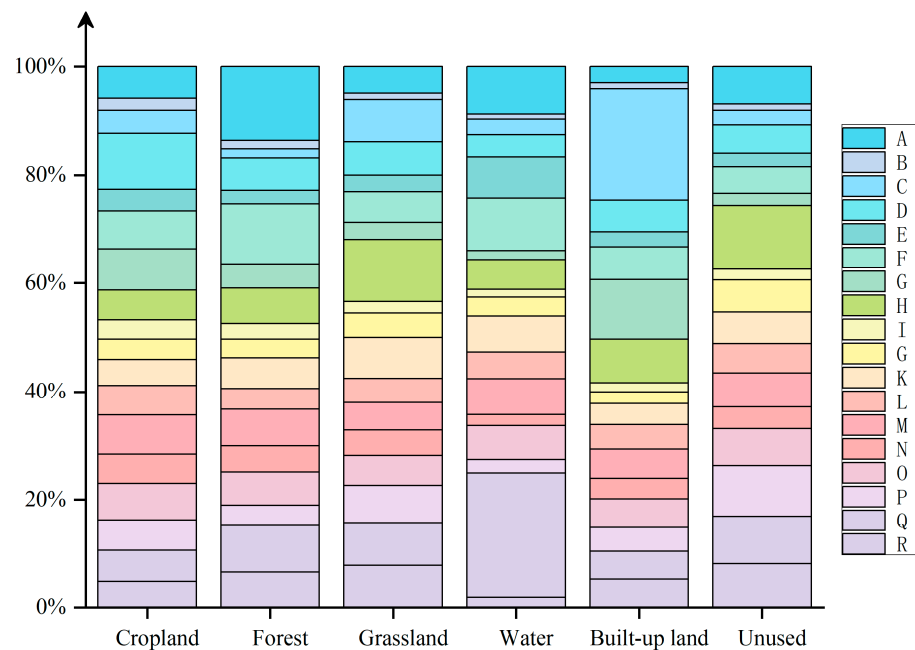

Figure 12. Contribution map of driving factors of environmental quality in 2020. A: DEM; B: GDP; C: night lights; D: NDVI; E: NPP; F: potential evapotranspiration; G: population; H: rainfall; I: slope; J: soil type; K: temperature; L: distance from the 1st-class road; M: distance from the 2nd-class road; N: distance from the 3rd-class road; O: distance from highway; P: distance from railway; Q: distance from water; R: distance from county seat.

4.6. Analysis of Cold and Hot Spots

Figure 13 depicts the hot and cold spots of spatial distributions for HQ in the THB from 1990 to 2050 (under three different scenarios). It reveals a distinct clustering pattern of HQ in the study area, with a relatively balanced distribution of hot and cold spots. However, over time, not only does the hot spot area expand, but it also gains increased confidence. Furthermore, the predictions for the three scenarios in 2050 further accentuate this trend, revealing the diffusion of hot spots at different confidence levels. In particular, under the EP scenario, hot spots may cover a broader area at a 99% confidence level. They are primarily located in the Bogda Peak Mountains of the eastern segment of the North Tianshan Mountains and the Jueluotage Mountains of the middle and eastern segments, showing a clustered distribution along mountain ranges. Cold spots tend to aggregate in unused areas, and 90% of the regions showing no significant changes are located in these unused areas. In addition, the spatial distribution of hot spots indicated by HQ levels in the Turpan Basin aligns closely with the distribution pattern of high-value spatial regions, while the distribution of cold spots matches that of low-value spatial regions. Hot spot areas accounted for 23.04% in 1990, increased to 26.18% in 2020, peaked at 26.78% in 2010, and decreased by 0.6% from 2010 to 2020. Cold spot areas exhibited a continuously increasing trend spanning 1990~2020, signifying a deterioration in HQ within low-value areas. In 2050, hot spots under all three scenarios show a decreasing trend, among which the UD scenario exhibits the lowest percentage of hot spots at 16.33% and the EP scenario exhibits

the lowest percentage of cold spots at 28.81%. The majority of regions with insignificant changes exhibit similar spatial distribution characteristics to both high- and low-value areas of HQ.
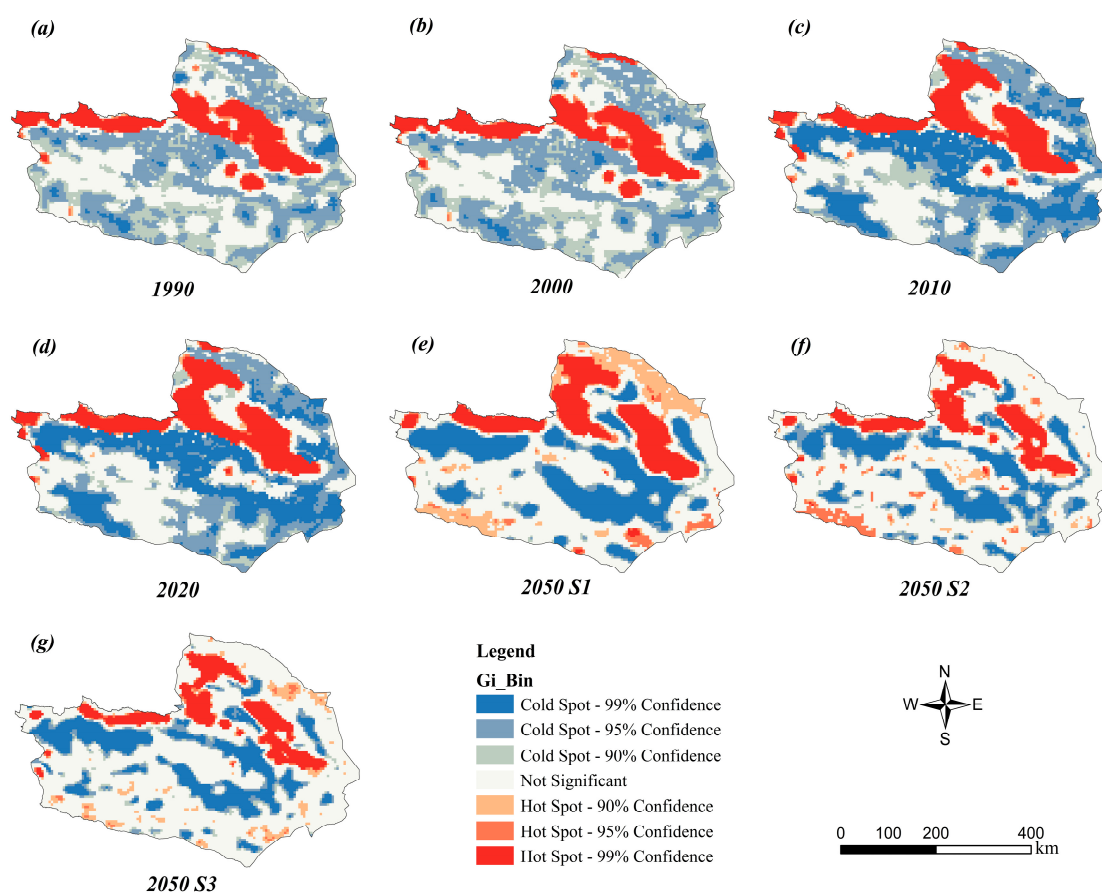
Figure 13. Distribution of hot spots of HQ in the THB at different times: (**a**) 1990, (**b**) 2000, (**c**) 2010, (**d**) 2020. Distribution of hot spots of HQ for the three scenarios in 2050: (**e**) ND; (**f**) UD; (**g**) EP.

5. Discussion

5.1. Response Mechanism of HQ to Land Use

Researchers have long focused on the relationship between HQ and land use [46,47]. In recent decades, urbanization has accelerated, exacerbating the scarcity of land resources [48]. The loss of ecosystem services has escalated in tandem with the rapid pace of land development [49,50]. The THB exhibits a typical continental arid climate, representing an extremely arid region. The ecosystem in this area is highly delicate and possesses weak environmental resilience. Once the ecological environment is compromised, restoration to its previous state becomes challenging. Multiple factors collectively contribute to the variations in land use patterns, with cultivated land, urban areas, and unused land posing threats to HQ. Changes in the extent across various land use types directly impact the quality of habitats. In the case of land use transitions, the period between 2000 and 2010 exhibited the most significant land shifts. Unused land notably decreased, while farmland, grassland, and urban areas experienced substantial increases. Specifically, the transition from unused land to grassland covered an area of 4803.51 km^2, and the transition from grassland to forest land amounted to 427.74 km^2. These trends are closely associated with the implementation of national strategies such as the Western Development Program and ecological projects, the Three-North Shelterbelt Program, the Grain for Green Project, and the Grazing Withdrawal and Grassland Restoration Project. The average HQ also improved from 0.110 in 2000 to 0.129 in 2010. Research indicates that natural vegetation significantly contributes to HQ restoration. Concurrently, urban expansion has been linked to HQ degra-

dation [51–53]. These findings are consistent with the rapid urban development observed during 2010–2020.

5.2. Changes in HQ Under Different Future Scenarios

To assess the impact of ecological development and urbanization on HQ, we conducted simulations and compared changes in HQ for the three scenarios in 2050. The findings revealed that the most significant decline in HQ occurred under the UD scenario. The primary cause lies in the unregulated expansion of built-up areas, destroying forest, grassland, and water bodies, thereby posing a threat to biodiversity's living environment. Excessive urban expansion also negatively affects water resource availability and water environment protection, consequently constraining economic development and construction activities within the THB. The EP scenario leads to a significant enhancement in HQ, primarily attributed to the expansion of ecological land, including forest, grassland, and water bodies. This expansion promotes ecosystem stability and aligns with previous research findings [54–56]. The development of land use types is closely intertwined with climate factors [57]. Upon investigating the drivers behind the growth of various land use types, it is evident that precipitation, potential evaporation, and temperature are pivotal factors influencing the development of grassland, forest, water bodies, and unused land, which highlights the importance of climate factors in driving changes in HQ. The THB is a critical region constrained by limited water resources, which in turn restricts both the advancement of the economy and the preservation of ecological integrity. Upon comparing the simulation results of the three scenarios, opting for the UD scenario, characterized by significant built-up land expansion, is not advisable. Conversely, the EP scenario falls short of fulfilling economic development objectives. In light of the THB's ecological fragility and severe water shortage, maintaining a balance between urban progress and ecological protection becomes crucial. This can be achieved rationally by controlling the increase in built-up land, protecting or appropriately increasing ecological land, and promoting green urbanization construction, so as to address the equilibrium between economic development and ecological conservation for sustainable growth in the THB.

5.3. Limitations of the Study

This work studies the dynamics of habitat quality (HQ) degradation and spatial distribution in the Turpan–Hami Basin from 1990 to 2050 using the InVEST model to evaluate historical changes and the PLUS-InVEST coupling model to predict future scenarios However, certain limitations need to be acknowledged. Given the unique land use patterns observed in the THB, where a significant proportion of land remains unused, overall changes in HQ may not be substantial. Furthermore, the calculation of HQ relies on subjective parameters associated with the selection of land use types and threat source suitability. Subsequent research endeavors will integrate more detailed remote sensing data analysis for each specific land type while exploring the relationship between driving factors and HQ. Additionally, future studies will expand to include time-series analysis of remote sensing data, multi-factor driver analysis, and high-resolution satellite imagery to refine the understanding of land use impacts on HQ. GIS-based spatial analysis and ecological modeling will also be employed to assess spatial patterns and predict HQ under different land use scenarios. Furthermore, socio-economic factors, as well as future land use planning scenarios, will be incorporated to provide a comprehensive view of land management's role in shaping habitat quality. Additionally, future research will explore the coupling of ecosystem service flows from various dimensions, investigating how different ecosystem services interact and contribute to overall ecological health and resilience in the region.

6. Conclusions

This study examines the spatiotemporal dynamics of the HQ by means of the InVEST-PLUS model, identifies the hot and cold spots of HQ in the THB spanning 1990 to 2020, and predicts the situations from 1990 to 2050. The derived conclusions are as follows:

1. Thank you, modified to this form of serial number, please check out1. Over the past three decades, cultivated land, grassland, and built-up land within the THB have been on an upward trend. Conversely, forests, water bodies, and unused land have exhibited a declining trend. Notably, built-up land has experienced the most substantial increase, leading to significant alterations in the spatial distribution pattern of HQ between 1990 and 2020.

2. The ecological environment within the THB is relatively fragile, and the overall HQ is low. Spatial clustering of HQ is evident across areas, and areas with high HQ are primarily concentrated along the Tianshan Mountains where grassland and forest play a significant role.

3. Unused land dominates the landscape composition of the THB; therefore, different patterns of land usage significantly influence the variations in HQ dynamics. The UD scenario results in severe degradation of HQ while the EP scenario greatly enhances the HQ.

The discoveries of this study can aid policymakers in obtaining a more profound comprehension of the urgency and critical areas for habitat protection. Additionally, they can aid in the timely detection of changing trends in HQ, warning against potential ecological risks, and developing corresponding strategies and management measures to optimize HQ. This study offers valuable insights for ecological regionalization planning and upgrading of HQ in arid regions.

Author Contributions: Y.L. (Yaqian Li): writing—original draft, methodology, formal analysis, visualization. Y.L. (Yongqiang Liu): data collection, methodology, writing—review and editing, funding acquisition, supervision. Y.Q. methodology, writing—review and editing. K.Z.: writing—review and editing. R.E.: writing—review and editing. W.W.: writing—review and editing. S.Y.: writing—review and editing. All authors have read and agreed to the published version of the manuscript.

Data Availability Statement: The datasets used and analyzed during the current study are available from the corresponding author on reasonable request.

Conflicts of Interest: The authors declare that they have no known competing financial interests or personal relationships that could impact the work reported in this paper.

References

1. He, B.; Chang, J.; Guo, A.; Wang, Y.; Wang, Y.; Li, Z. Assessment of river basin habitat quality and its relationship with disturbance factors: A case study of the Tarim River Basin in Northwest China. *J. Arid Land.* **2022**, *14*, 167–185. [CrossRef]
2. Rands, M.R.; Adams, W.M.; Bennun, L.; Butchart, S.H.; Clements, A.; Coomes, D.; Entwistle, A.; Hodge, I.; Kapos, V.; Scharlemann, J.P.; et al. Biodiversity conservation: Challenges beyond 2010. *Science* **2010**, *329*, 1298–1303. [CrossRef] [PubMed]
3. Dai, L.; Li, S.; Lewis, B.J.; Wu, J.; Yu, D.; Zhou, W.; Zhou, L.; Wu, S. The influence of land use change on the spatial–temporal variability of habitat quality between 1990 and 2010 in Northeast China. *J. For. Res.* **2019**, *30*, 2227–2236. [CrossRef]
4. Hales, S.; Butler, C.; Woodward, A.; Corvalan, C. Health Aspects of the Millennium Ecosystem Assessment. *Ecohealth* **2004**, *1*, 124–128. [CrossRef]
5. Bai, L.; Xiu, C.; Feng, X.; Liu, D. Influence of urbanization on regional habitat quality: A case study of Changchun City. *Habitat Int.* **2019**, *93*, 102042. [CrossRef]
6. Tang, F.; Fu, M.; Wang, L.; Zhang, P. Land-use change in Changli County, China: Predicting its spatio-temporal evolution in habitat quality. *Ecol. Indic.* **2020**, *117*, 106719. [CrossRef]

7. Zhang, X.; Song, W.; Lang, Y.; Feng, X.; Yuan, Q.; Wang, J. Land use changes in the coastal zone of China's Hebei Province and the corresponding impacts on habitat quality. *Land Use Policy* **2020**, *99*, 104957. [CrossRef]

8. Zhang, H.; Lang, Y. Quantifying and Analyzing the Responses of Habitat Quality to Land Use Change in Guangdong Province, China over the Past 40 Years. *Land* **2022**, *11*, 817. [CrossRef]

9. Riedler, B.; Pernkopf, L.; Strasser, T.; Lang, S.; Smith, G. A composite indicator for assessing habitat quality of riparian forests derived from Earth observation data. *Int. J. Appl. Earth Obs. Geoinf.* **2015**, *37*, 114–123. [CrossRef]

10. Riedler, B.; Lang, S. A spatially explicit patch model of habitat quality, integrating spatio-structural indicators. *Ecol. Indic.* **2018**, *94*, 128–141. [CrossRef]

11. Liao, J.; Zhang, D.; Su, S.; Liang, S.; Du, J.; Yu, W.; Ma, Z.; Chen, B.; Hu, W. Coastal habitat quality assessment and mapping in the terrestrial-marine continuum: Simulating effects of coastal management decisions. *Ecol. Indic.* **2023**, *156*, 111158. [CrossRef]

12. Hasan, S.S.; Zhen, L.; Miah, M.G.; Ahamed, T.; Samie, A. Impact of land use change on ecosystem services: A review. *Environ. Dev.* **2020**, *34*, 100527. [CrossRef]

13. Li, J.; Zhang, C.; Zhu, S. Relative contributions of climate and land-use change to ecosystem services in arid inland basins. *J. Clean. Prod.* **2021**, *298*, 126844. [CrossRef]

14. Janus, J.; Bozek, P. Land abandonment in Poland after the collapse of socialism: Over a quarter of a century of increasing tree cover on agricultural land. *Ecol. Eng.* **2019**, *138*, 106–117. [CrossRef]

15. Yang, Y. Evolution of habitat quality and association with land-use changes in mountainous areas: A case study of the Taihang Mountains in Hebei Province, China. *Ecol. Indic.* **2021**, *129*, 107967. [CrossRef]

16. Zhao, Q.; Shao, J. Evaluating the impact of simulated land use changes under multiple scenarios on ecosystem services in Ji'an, China. *Ecol. Indic.* **2023**, *156*, 111040. [CrossRef]

17. Zeng, J.; Wu, J.; Chen, W. Coupling analysis of land use change with landscape ecological risk in China: A multi-scenario simulation perspective. *J. Clean. Prod.* **2024**, *435*, 140518. [CrossRef]

18. Wang, J.; Liu, Y.; Liu, Z. Spatio-Temporal Patterns of Cropland Conversion in Response to the "Grain for Green Project" in China's Loess Hilly Region of Yanchuan County. *Remote Sens.* **2013**, *5*, 5642–5661. [CrossRef]

19. Tariq, A.; Yan, J.; Mumtaz, F. Land change modeler and CA-Markov chain analysis for land use land cover change using satellite data of Peshawar, Pakistan. *Phys. Chem. Earth Parts A/B/C* **2022**, *128*, 103286. [CrossRef]

20. Qian, Y.; Xing, W.; Guan, X.; Yang, T.; Wu, H. Coupling cellular automata with area partitioning and spatiotemporal convolution for dynamic land use change simulation. *Sci. Total Environ.* **2020**, *722*, 137738. [CrossRef] [PubMed]

21. Zhang, X.; Ren, W.; Peng, H. Urban land use change simulation and spatial responses of ecosystem service value under multiple scenarios: A case study of Wuhan, China. *Ecol. Indic.* **2022**, *144*, 109526. [CrossRef]

22. Zhang, Z.; Li, X.; Liu, X.; Zhao, K. Dynamic simulation and projection of land use change using system dynamics model in the Chinese Tianshan mountainous region, central Asia. *Ecol. Model.* **2024**, *487*, 110564. [CrossRef]

23. Wang, B.; Yang, T. Assessing Impact of Land Use Change on the Ecosystem Service Value in Yinchuan City from 1980 to 2018. *Sustainability* **2021**, *13*, 8311. [CrossRef]

24. Zhao, J.; Shao, Z.; Xia, C.; Fang, K.; Chen, R.; Zhou, J. Ecosystem services assessment based on land use simulation: A case study in the Heihe River Basin, China. *Ecol. Indic.* **2022**, *143*, 109402. [CrossRef]

25. Feng, X.; Li, Y.; Wang, X.; Yang, J.; Yu, E.; Wang, S.; Wu, N.; Xiao, F. Impacts of land use transitions on ecosystem services: A research framework coupled with structure, function, and dynamics. *Sci. Total Environ.* **2023**, *901*, 166366. [CrossRef]

26. Sallustio, L.; De Toni, A.; Strollo, A.; Di Febbraro, M.; Gissi, E.; Casella, L.; Geneletti, D.; Munafò, M.; Vizzarri, M.; Marchetti, M. Assessing habitat quality in relation to the spatial distribution of protected areas in Italy. *J. Environ. Manage.* **2017**, *201*, 129–137. [CrossRef]

27. Meimei, W.; Zizhen, J.; Tengbiao, L.; Yongchun, Y.; Zhuo, J. Analysis on absolute conflict and relative conflict of land use in Xining metropolitan area under different scenarios in 2030 by PLUS and PFCI. *Cities* **2023**, *137*, 104314. [CrossRef]

28. Gao, L.; Tao, F.; Liu, R.; Wang, Z.; Leng, H.; Zhou, T. Multi-scenario simulation and ecological risk analysis of land use based on the PLUS model: A case study of Nanjing. *Sust. Cities Soc.* **2022**, *85*, 104055. [CrossRef]

29. Zhang, Z.; Zhang, H.; Feng, J.; Wang, Y.; Liu, K. Evaluation of Social Values for Ecosystem Services in Urban Riverfront Space Based on the SolVES Model: A Case Study of the Fenghe River, Xi'an, China. *Int. J. Environ. Res. Public Health* **2021**, *18*, 2765. [CrossRef] [PubMed]

30. Sherrouse, B.C.; Semmens, D.J.; Clement, J.M. An application of Social Values for Ecosystem Services (SolVES) to three national forests in Colorado and Wyoming. *Ecol. Indic.* **2014**, *36*, 68–79. [CrossRef]

31. Aznarez, C.; Jimeno-Sáez, P.; López-Ballesteros, A.; Pacheco, J.P.; Senent-Aparicio, J. Analysing the Impact of Climate Change on Hydrological Ecosystem Services in Laguna del Sauce (Uruguay) Using the SWAT Model and Remote Sensing Data. *Remote Sens.* **2021**, *13*, 2014. [CrossRef]

32. Kim, Y.; Lee, J.; Woo, S.; Lee, J.; Hur, J.; Kim, S. Design of Ecological Flow (E-Flow) Considering Watershed Status Using Watershed and Physical Habitat Models. *Water* **2023**, *15*, 3267. [CrossRef]

33. Chen, M.; Fan, H.; Zhang, X.; Lai, F.; Jia, X.; Huang, T.; Liu, Y. Spatial–Temporal Evolution and Driving Factors of HQ in Malus sieversii Forest Areas in the Western Tianshan Mountain's Watersheds. *Forests* **2023**, *14*, 104. [CrossRef]

34. Zhang, T.; Chen, Y. The effects of landscape change on HQ in arid desert areas based on future scenarios: Tarim River Basin as a case study. *Front. Plant Sci.* **2022**, *13*, 1031859.

35. Wang, H.; Hu, Y.; Yan, H.; Liang, Y.; Guo, X.; Ye, J. Trade-off among grain production, animal husbandry production, and HQ based on future scenario simulations in Xilinhot. *Sci. Total Environ.* **2022**, *817*, 153015. [CrossRef]

36. Wei, Q.; Abudureheman, M.; Halike, A.; Yao, K.; Yao, L.; Tang, H.; Tuheti, B. Temporal and spatial variation analysis of habitat quality on the PLUS-InVEST model for Ebinur Lake Basin, China. *Ecol. Indic.* **2022**, *145*, 109632. [CrossRef]

37. Wang, B.; Oguchi, T.; Liang, X. Evaluating future habitat quality responding to land use change under different city compaction scenarios in Southern China. *Cities* **2023**, *140*, 104410. [CrossRef]

38. Liu, Y.; Jing, Y.; Han, S. Multi-scenario simulation of land use/land cover change and water yield evaluation coupled with the GMOP-PLUS-InVEST model: A case study of the Nansi Lake Basin in China. *Ecol. Indic.* **2023**, *155*, 110926. [CrossRef]

39. Li, Z.; Chen, X.; Qi, J.; Xu, C.; An, J.; Chen, J. Accuracy assessment of land cover products in China from 2000 to 2020. *Sci. Rep.* **2023**, *13*, 12936. [CrossRef]

40. Cheng, W.; Feng, Q.; Xi, H.; Yin, X.; Sindikubwabo, C.; Habiyakare, T.; Chen, Y.; Zhao, X. Spatiotemporal variability and controlling factors of groundwater depletion in endorheic basins of Northwest China. *J. Environ. Manage* **2023**, *344*, 118468. [CrossRef]

41. Wei, H.; Liu, H.; Xu, Z.; Ren, J.; Lu, N.; Fan, W.; Zhang, P.; Dong, X. Linking ecosystem services supply, social demand and human well-being in a typical mountain–oasis–desert area, Xinjiang, China. *Ecosyst. Serv.* **2018**, *31*, 44–57. [CrossRef]

42. Goldstein, J.H.; Caldarone, G.; Duarte, T.K.; Ennaanay, D.; Hannahs, N.; Mendoza, G.; Polasky, S.; Wolny, S.; Daily, G.C. Integrating ecosystem-service tradeoffs into land-use decisions. *Proc. Natl. Acad. Sci. USA* **2012**, *109*, 7565–7570. [CrossRef] [PubMed]

43. Sun, X.; Jiang, Z.; Liu, F.; Zhang, D. Monitoring spatio-temporal dynamics of habitat quality in Nansihu Lake basin, eastern China, from 1980 to 2015. *Ecol. Indic.* **2019**, *102*, 716–723. [CrossRef]

44. Liang, X.; Guan, Q.; Clarke, K.C.; Liu, S.; Wang, B.; Yao, Y. Understanding the drivers of sustainable land expansion using a patch-generating land use simulation (PLUS) model: A case study in Wuhan, China. *Comput. Environ. Urban Syst.* **2021**, *85*, 101569. [CrossRef]

45. Wang, H.; Yuan, W.; Ma, Y.; Bai, X.; Huang, L.; Cheng, S.; Yang, H.; Guo, W. Spatiotemporal dislocation of ecosystem supply and demand services from habitat quality under different development scenarios. *Ecol. Indic.* **2023**, *157*, 111230. [CrossRef]

46. Gao, Y.; Ma, L.; Liu, J.; Zhuang, Z.; Huang, Q.; Li, M. Constructing Ecological Networks Based on HQ Assessment: A Case Study of Changzhou, China. *Sci. Rep.* **2017**, *7*, 46073.

47. Wu, Y.; Tao, Y.; Yang, G.; Ou, W.; Pueppke, S.; Sun, X.; Chen, G.; Tao, Q. Impact of land use change on multiple ecosystem services in the rapidly urbanizing Kunshan City of China: Past trajectories and future projections. *Land Use Policy* **2019**, *85*, 419–427. [CrossRef]

48. Chen, G.; Li, X.; Liu, X.; Chen, Y.; Liang, X.; Leng, J.; Xu, X.; Liao, W.; Qiu, Y.A.; Wu, Q.; et al. Global projections of future urban land expansion under shared socioeconomic pathways. *Nat. Commun.* **2020**, *11*, 537. [CrossRef]

49. Aziz, T. Changes in land use and ecosystem services values in Pakistan, 1950–2050. *Environ. Dev.* **2021**, *37*, 100576. [CrossRef]

50. He, N.; Guo, W.; Wang, H.; Yu, L.; Cheng, S.; Huang, L.; Jiao, X.; Chen, W.; Zhou, H. Temporal and Spatial Variations in Landscape Habitat Quality under Multiple Land-Use/Land-Cover Scenarios Based on the PLUS-InVEST Model in the Yangtze River Basin, China. *Land* **2023**, *12*, 1338. [CrossRef]

51. HE, C.; LIU, Z.; TIAN, J.; MA, Q. Urban expansion dynamics and natural habitat loss in China: A multiscale landscape perspective. *Glob. Change Biol.* **2014**, *20*, 2866–2902. [CrossRef]

52. Han, P.; Xiang, J.; Zhao, Q. Spatial differentiation and scenario simulation of cultivated land in mountainous areas of Western Hubei, China: A PLUS model. Environ. *Sci. Pollut. Res.* **2023**, *30*, 52804–52817. [CrossRef]

53. Wu, J.; Li, X.; Luo, Y.; Zhang, D. Spatiotemporal effects of urban sprawl on habitat quality in the Pearl River Delta from 1990 to 2018. *Sci. Rep.* **2021**, *11*, 13981. [CrossRef] [PubMed]

54. Wu, J.; Luo, J.; Zhang, H.; Qin, S.; Yu, M. Projections of land use change and habitat quality assessment by coupling climate change and development patterns. *Sci. Total Environ.* **2022**, *847*, 157491. [CrossRef]

55. Peng, Y.; Cheng, W.; Xu, X.; Song, H. Analysis and prediction of the spatiotemporal characteristics of land-use ecological risk and carbon storage in Wuhan metropolitan area. *Ecol. Indic.* **2024**, *158*, 111432. [CrossRef]

56. He, J.; Huang, J.; Li, C. The evaluation for the impact of land use change on habitat quality: A joint contribution of cellular automata scenario simulation and habitat quality assessment model. *Ecol. Model.* **2017**, *366*, 58–67. [CrossRef]

57. Peters, M.K.; Hemp, A.; Appelhans, T.; Becker, J.N.; Behler, C.; Classen, A.; Detsch, F.; Ensslin, A.; Ferger, S.W.; Frederiksen, S.B.; et al. Climate–land-use interactions shape tropical mountain biodiversity and ecosystem functions. *Nature* **2019**, *568*, 88–92. [CrossRef] [PubMed]